

**Article type:** Original article

**Global pattern of interkinetic nuclear migration in tracheoesophageal epithelia of the mouse embryo: inter-organ and intra-organ regional differences.**

**First author's surname:** Getachew

Dereje Getachew<sup>1</sup>, Akihiro Matsumoto<sup>1</sup>, Yasuhiro Uchimura<sup>2</sup>, Jun Udagawa<sup>2</sup>, Nanako Mita<sup>1</sup>, Noriko Ogawa<sup>1</sup>, Shigeru Moriyama<sup>1</sup>, Akiyasu Takami<sup>3</sup>, Hiroki Otani<sup>1\*</sup>

1) Department of Developmental Biology, Faculty of Medicine, Shimane University

2) Department of Anatomy, Shiga University of Medical Science

3) Department of Mechanical Engineering, National Institute of Technology, Matsue College

**Short title: INM in trachea and esophagus**

**\*Corresponding author:** Hiroki Otani, Department of Developmental Biology, Faculty of Medicine, Shimane University, 89-1 Enya-Cho, Izumo, Shimane 693-8501, Japan.

Phone: +81-853-20-2102; Fax: +81-853-20-2100; Email: hotani@med.shimane-u.ac.jp

## **Abstract**

Interkinetic nuclear migration (INM) is an apicobasal (AB) polarity-based regulatory mechanism of proliferation/differentiation in epithelial stem/progenitor cells. We previously documented INM in the endoderm-derived tracheal/esophageal epithelia at embryonic day (E) 11.5 and suggested that INM is involved in the development of both organs. We here investigated inter-organ (trachea *vs.* esophagus) and intra-organ regional (ventral *vs.* dorsal) differences in the INM mode in the tracheal and esophageal epithelia of the mouse embryo. We also analyzed convergent extension (CE) and planar cell movement (PCM) in the epithelia based on cell distribution. The pregnant C57BL/6J mice were intraperitoneally injected with 5-ethynyl-2'-deoxyuridine at E11.5 and E12.5 and were sacrificed 1, 4, 6, 8 and 12 hr later to obtain the embryos. The distribution of labeled cell nuclei along the AB axis was chronologically analyzed in the total, ventral and dorsal sides of the epithelia. The percentage distribution of the nuclei population was represented by histogram and the chronological change was analyzed statistically using multi-dimensional scaling. The inter-organ comparison of the INM mode during E11.5–E12.0, but not E12.5–E13.0, showed a significant difference. During E11.5–E12.0 the trachea, but not the esophagus, showed a significant difference between ventral and dorsal sides. During E12.5–E13.0 neither organ showed regional differences. CE appeared to occur in both organs during E11.5–E12.0 while PCM was unclear in both organs. These findings suggest a difference between the trachea and esophagus, and a regional difference in the trachea, not in the esophagus, in the INM mode, which may be related with the later differential organogenesis/histogenesis of these organs.

**Keywords:** trachea, esophagus, interkinetic nuclear migration, inter-organ, regional difference

## INTRODUCTION

The trachea and esophagus start to develop from the common anterior foregut at embryonic day (E) 9.5 in mice, and the separation into the ventral trachea and dorsal esophagus is almost complete before E11.5.<sup>1</sup> Epithelial expression of the transcription factors Nkx2.1 and Sox2 and the related signaling molecules has been shown to be essentially involved in the separation and further development of the trachea and esophagus (for review, see Wong et al. 2016).<sup>2</sup> Experimental disruption of the expression of these transcription factors and the signaling pathways leads to the formation of esophageal atresia with/without fistula (EA/TEF) (for review, see Wong et al. 2016),<sup>2</sup> which is a relatively common birth defect with an incidence rate of 1/3500 in humans. In spite of these findings on the final determination/perturbation of organ identities, the cellular events in these normal and abnormal processes remain largely unknown.

These previous studies described that the epithelial lining of both the trachea and esophagus is “simple” columnar when they are separated from each other, and that the tracheal epithelium remains the same, whereas the esophageal epithelium changes into stratified squamous during the course of development (for review, see Wong et al. 2016).<sup>2</sup> However, we have recently proved that this classic description of the epithelial structure of the two organs is not strictly accurate. The epithelia of the trachea and esophagus are not “simple” columnar but “pseudostratified” columnar, which is a hallmark of the epithelia in which the interkinetic nuclear migration (INM) works as a regulatory mechanism of epithelial proliferation and differentiation.<sup>3</sup> We further reported that transient and dynamic morphologic changes involving the cytoskeleton and cell-adhesion apparatus occur in the

esophageal epithelium in close relation with the cessation of INM and transition into the stratified squamous structure.<sup>3</sup>

INM is the apicobasal (AB) cell polarity-based oscillatory movement of epithelial cell nuclei that is synchronized with the progression of the cell cycle, i.e., the M-phase at the apical surface and S-phase at the basal side, and thus generates the pseudostratified structure of the epithelium.<sup>4-9</sup> It has been suggested that INM maximizes the number of mitoses at the limited apical surface to allow efficient stem/progenitor cell expansion.<sup>6,10</sup> However, the exact developmental function of INM remains controversial.<sup>11</sup> While INM has been extensively studied in brain/neuroectoderm development,<sup>6-11</sup> recent studies including ours have documented INM in other endoderm- and mesoderm-derived epithelia.<sup>4,12-15</sup> We reported the INM throughout the entire intestine, trachea and esophagus of endoderm origin, and ureter of mesoderm origin in mice.<sup>12-15</sup> We statistically analyzed the chronological change in the distribution patterns of labeled proliferating cell nuclei along the AB axis in these epithelia, proved the existence of INM, and further revealed different modes of INM between the different organs, different parts of the intestine, and different dates of development of the same organ.<sup>14,15</sup> Therefore, INM through these differential modes could regulate the total number and the localized distribution of stem/progenitor and the resultant daughter cells, and thus the size and shape of the organs.<sup>15,16</sup> Regarding the trachea and esophagus, we previously showed the existence of INM during E11.5–E12.0,<sup>12</sup> but detailed analysis of the INM mode on the inter-organ and intra-organ regional differences has not yet been done. The trachea has a clear structural difference between the ventral and dorsal sides, while in the esophagus there is no apparent structural difference between the ventral and dorsal sides. Thus, we

hypothesized that the INM mode may be different between the two organs and between the ventral and dorsal sides in the trachea.

We also previously showed that a convergent extension (CE) mechanism is involved in the elongation of the midgut,<sup>17,18</sup> in which epithelial cell nuclei are rearranged to converge toward the center of the gut, causing extension of the gut along its long (L) axis which is perpendicular to the epithelial AB axis.<sup>19,20</sup> Further, cell movement in planar cell polarity (PCP) (planar cell movement: PCM) has been documented as a basic cellular event that plays important roles in the development of tissues and organs (for review, see Davey and Moens 2017; Henderson et al. 2018).<sup>21,22</sup> Therefore, in addition to INM, CE and PCM should be simultaneously examined as morphogenic cellular events in the development of tracheal and esophageal epithelia.

In the present study, we first investigated the existence of INM in the epithelium of the trachea and esophagus using two consecutive developmental ages of mice during E11.5–E12.0 and E12.5–E13.0. Then the results were comparatively analyzed to determine whether similarities or dissimilarities, i.e. inter-organ and intra-organ regional differences, exist in the INM mode. We used already established laboratory methods presented in our previous series of studies (see Methods section).<sup>12–15</sup> We concurrently indirectly investigated CE using the chronological measurement of total cell distribution along the L axis of the epithelial tube and PCM using the chronological measurement of % distribution of labeled nuclei along the L axis.

## MATERIALS AND METHODS

### Animals

C57BL/6J mice (CLEA Japan, Tokyo) between 8 and 20 weeks of age were used. The mice were housed in the Department of Experimental Animals, Interdisciplinary Center for Science Research, Organization for Research and Academic Information, Shimane University. They were kept under conditions of constant temperature and humidity, and a controlled 12/12 hr light-dark cycle. They were given a standard laboratory diet and water, both *ad libitum*. Single potent male and female mice were mated at night around 22:00 in the same cage, and the presence of a vaginal plug was checked at midnight, which was defined as E0.0. This study was approved by the Ethics Committee for Animal Experimentation of Shimane University, and the animals were handled in accordance with the institutional guidelines.

### EdU labeling assay

At E11.5 and E12.5, the pregnant mice received a single intraperitoneal injection of 5-ethynyl-2'-deoxyuridine (EdU; Invitrogen, Carlsbad, CA; 30 mg/kg). Then, at each of 1, 4, 6, 8, and 12 hr after EdU injection, three of the mice were sacrificed by injecting 0.5 ml of pentobarbital sodium, which is an overdose for euthanasia, and one embryo was obtained from each, for a total of 30 embryos. The embryos were fixed in 4% formaldehyde/70% methanol overnight at 4°C. After dehydration in a graded series of ethanol, the embryos were embedded in paraffin and sectioned horizontally at 5 µm thickness. The sections were deparaffinized and rehydrated in a graded series of ethanol. They were then washed with tris-buffered saline (TBS)/0.03% Triton® X-100 for permeabilization of the cell membrane. Finally, the EdU-labeled nuclei were stained using a Click-iT™ EdU Cell Proliferation Kit

for Imaging, Alexa Fluor<sup>TM</sup> 488 dye (Invitrogen, Carlsbad, CA), and the nuclei were stained with 4', 6-diamidino-2-phenylindole (DAPI; Dojindo, Kumamoto, Japan). The micrographic images were taken using a Keyence BZ-X700 series all-in-one fluorescence microscopy (Keyence, Osaka, Japan). We counted the total cell nuclei using ImageJ (National Institutes of Health, Bethesda, Maryland, USA).

### **Measurement of nuclear distribution along the AB axis**

Sections from the level of separation of the foregut into the trachea and esophagus to the level proximal to the bifurcation of the trachea were examined in the following analyses, and therefore the distal (stomach side) part of the esophagus below the level of the tracheal bifurcation was not involved in the present study. The EdU-positive nuclei distribution between the apical and basal surfaces in the tracheal and esophageal epithelia were measured in 5  $\mu\text{m}$  thick horizontal serial sections every 30  $\mu\text{m}$  for E11.5 and every 50  $\mu\text{m}$  for E12.5, using an image analysis program as reported previously (Fig. 1).<sup>12,13,15</sup> The image analysis program divides the epithelial layer into six equal concentric layers (L1–L6) at interval of 15° segments each (Fig. 1A). We set up the outermost circle at the basal side corresponding to the basement membrane which faces the mesenchymal tissue (basal side, L1) and the innermost circle at the apical surface corresponding to the lumen of the epithelium which faces the free surface (apical side, L6).<sup>12,13,15</sup> Then, to count the position of the EdU-positive nuclei applied to six layers, we placed a dot at the center of each nucleus and then determined the layer to which it belongs (Fig. 1B). The numbers of EdU-positive nuclei counted per sample per each time point were 847–1300 for E11.5–E12.0 and 1217–2056 for E12.5–E13.0 for the trachea, and 531–1039 for E11.5–E12.0 and 1053–1613 for E12.5–E13.0 for the

esophagus. The EdU-positive nuclei in each layer at each time point were represented using a % population histogram showing means plus SD values.

### **Cell number and EdU-positive/negative nuclei number counts**

To examine CE and PCM indirectly from the change in the cell number distribution and in the ratio of EdU-positive nuclei along the L axis of the trachea and esophagus, respectively, the cell number and number of EdU-positive/negative nuclei in the sections were counted using ImageJ software.

### **Statistical analysis**

We analyzed the patterns of histogram at each time point using multidimensional scaling (MDS). MDS is a method for the statistical analysis of multidimensional information on a two-dimensional (2D) graph that mathematically calculates similarities or dissimilarities among datasets in a large matrix. The EdU-positive nuclear distribution pattern in the histogram at each time point was plotted on a 2D plane. In the resulting graph, closer proximity was interpreted as greater similarity, and greater distance was interpreted as greater dissimilarity between time points.<sup>12,23,24</sup> The distance variation of each time point of the MDS results was further analyzed by using the MORPHOJ software package. MORPHOJ offers methods for studying morphologically integrated data.<sup>25,26</sup> We ran a one-way ANOVA to perform a canonical variate analysis (CVA), which is used to maximize the variation among specified groups. In our case, each time point was considered a distance distribution to compare as a group between the total trachea vs. total esophagus, and between the ventral vs. the dorsal sides of the two organs. The Procrustes distances among the groups were determined with the pairwise difference in means using permutation tests (10,000 rounds). A *P*-value < 0.05 was considered statistically significant.

## RESULTS

We used the EdU assay to label the DNA synthesis phase (S-phase) cell nuclei and to examine the distribution of labeled nuclei along the AB axis (Fig. 1). The *in vivo* intraperitoneally administered EdU was detected on a fixed histological tissue harvested at five different time points 1, 4, 6, 8, and 12 hr after the injection (Fig. 1D–F for E11.5 trachea, Fig. 1G–I for E11.5 esophagus, 1, 4, 12 hr each). The trachea and esophagus sections were taken at equal distance in proximal-to-distal fashion, from the separation of the foregut tube to the bifurcation of the trachea into two main bronchi, because the main goal of the project was to compare the INM mode between the trachea and esophagus. The distribution of the % of the EdU-positive nuclei population in layers L1–L6 at each time point was represented by histograms (Figs. 2–4, left panels) and then each time point was plotted on the 2D graph by using MDS (Figs. 2–4, right panels) to represent the similarities and dissimilarities among the histograms.

We comparatively analyzed the INM mode to determine the inter-organ difference between the trachea and esophagus during E11.5–E12.0 and E12.5–E13.0 (Fig. 2), and then to determine the intra-organ regional difference (ventral *vs.* dorsal) in each trachea (Fig. 3) and esophagus (Fig. 4) during E11.5–E12.0 and E12.5–E13.0.

### **The inter-organ difference in the INM mode between the trachea and esophagus**

During E11.5–E12.0, the population histograms for total trachea *vs.* total esophagus (Fig. 2A *vs.* 2B) both showed a similar general trend in the shift of distribution of the EdU-positive nuclei along the AB axis. The largest populations of DNA-synthesizing cells were observed

on the basal side (L1–L3) at 1 hr, and then they gradually shifted toward the apical side (L4–L5) at 4 hr and 6 hr, and finally shifted back to the basal side at 8 and 12 hr, thereby confirming the existence of INM. Whereas in the total esophagus the largest % of the EdU-positive nuclei appeared to remain on the basal side (L1–L3) even at the 4 hr and 6 hr time points (Fig. 2B), in the total trachea a significant portion of the population shifted to the apical side so that the size of the apical side population (L4–L6) became nearly identical to that of the basal side population (L1–L3) at 4 hr and 6 hr (Fig. 2A).

We then analyzed the histograms to determine the similarities and dissimilarities among them using MDS and plotted time points on the 2D plane. We interpreted the results in the same manner as in our previously published papers, i.e., on dimension 1, rightward corresponds to a basal side distribution shift of the nuclei population and leftward corresponds to an apical side shift.<sup>12-15</sup> During E11.5–E12.0, the total trachea (Fig. 2A) and total esophagus (Fig. 2B) showed generally similar patterns, with the 1 hr and 12 hr time points being located on the right (basal) side, while the 4 hr and 6 hr time points were on the left (apical) side and the 8 hr time point was in the middle of the 2D graph (Fig. 1A). The cell cycle was thus estimated to be 12 hr for both the total trachea and total esophagus. The basal-to-apical G2/M phase spanned 4 hr, and the return phase—i.e., the apical-to-basal G1 phase—took 8 hr for both organs (Fig. 2A, B). On the other hand, the distances between time points appeared somewhat different between the trachea and esophagus. To analyze whether this distance variation of each time point on the 2D graph between the two organs was statistically significant, we used CVA which discriminates against the variation among the time points (Fig. 5A). The shape difference in each group on the shape space was scattered on the two canonical variate axes (CV1 and CV2). The two canonical variates together accounted for 95.56% of the total

variation ( $CV_1 = 84.17\%$ ,  $CV_2 = 11.39\%$ ). The E11.5 scatter plot from  $CV_1$  and  $CV_2$  shows that each point from the two groups (total trachea *vs.* total esophagus) was clearly separated from the other on both the  $CV_1$  and  $CV_2$  axes (Fig. 5A). The Procrustes distance obtained by pairwise comparison among groups (the difference of means) was 0.4105, and this difference was highly statistically significant (permutation 10,000 rounds in MorphoJ:  $P < 0.0001$ ). Thus, the INM mode was interpreted as differing between the total trachea and total esophagus during E11.5–E12.0.

During E12.5–E13.0, the % of population histogram distributions for total trachea (Fig. 2C) *vs.* total esophagus (Fig. 2D) showed a trend similar to that of E11.5–E12.0 for both organs. In line with this finding, the 2D plots by MDS also showed a similarity of nuclei distribution at each time point, such that 1 hr and 12 hr were located on the right side and 4 hr and 6 hr were located on the left side. The cell cycle was again estimated to be 12 hr for both the total trachea and total esophagus. The basal-to-apical G2/M phase spanned 4–6 hr, whereas the return apical-to-basal phase took 6 hr for both the trachea and esophagus (Fig. 2C, D). At E12.5 the scatter plot from  $CV_1$  and  $CV_2$  shows that each time point from the two groups (total trachea *vs.* total esophagus) was separated from the other in the  $CV_1$  direction while the  $CV_2$  direction was overlapped (Fig. 5A). Thus the Procrustes distance obtained by pairwise comparison among the groups at E12.5 total trachea *vs.* total esophagus was 0.4325 and this difference was not statistically significant (permutation 10,000 rounds in MorphoJ:  $P < 0.0959$ ).

## **The intra-organ regional (ventral vs. dorsal) difference in the INM mode in the trachea and esophagus**

To analyze regional (ventral vs. dorsal) difference, we further divided the trachea and esophagus by using a ruler into two equal parts, the ventral and dorsal halves (Fig. 1C). The trachea corresponding to the esophagus side considered as dorsal and the opposite side as ventral and *vice versa* for the esophagus.

### **Trachea**

The E11.5–E12.0 and E12.5–E13.0 trachea histograms and MDS 2D graphs showed a general trend that proved the existence of INM with a cell cycle of 12 hr in both the ventral and dorsal halves (Fig. 3).

At a glance, the E11.5–E12.0 histograms and MDS 2D graphs exhibited some differences between the ventral and dorsal trachea (Fig. 3A vs. 3B), while the E12.5–E13.0 histograms and MDS 2D graphs looked very similar between the ventral and dorsal trachea (Fig. 3C vs. 3D). Together, the two canonical variates accounted for 98.40% of the total variation (CV1 = 62.99%, CV2 = 35.41%). The scatter plot from CV1 and CV2 shows that the two groups, ventral vs. dorsal trachea during E11.5–E12.0, were separated from each other on both CV1 and CV2 (Fig. 5B). Procrustes distance obtained by pairwise comparison among groups during E11.5–E12.0 trachea ventral vs. dorsal was 0.4036 and this difference was statistically significant (permutation 10,000 rounds in MorphoJ:  $P < 0.0123$ ). Thus, the INM mode is different between the ventral and dorsal trachea during E11.5–E12.0.

On the other hand, comparison of the trachea ventral vs. dorsal during E12.5–E13.0 revealed that the variation of the scatter plot at CV1 was overlapped between the two groups, while at CV2 the scatter plot variations of the two groups were separate from each other (Fig. 5B).

The Procrustes distance obtained by pairwise comparison among groups E12.5–E13.0 trachea ventral *vs.* dorsal was 0.2133, and this difference was not statistically significant (permutation 10,000 rounds in MorphoJ:  $P < 0.3025$ ).

### **Esophagus**

In the comparison between the ventral and dorsal portions of the esophagus at E11.5–E12.0, the distribution of labeled EdU-positive nuclei and mode of INM on MDS 2D graphs appeared to be quite similar (Fig. 4A, B). The two canonical variates together accounted for 98.81% of the total variation (CV1 = 91.07%, CV2 = 7.73%). The scatter plot from CV1 and CV2 shows that the two groups were overlapped during E11.5–E12.0 (Fig. 5C). The Procrustes distance obtained by pairwise comparison among groups between the ventral and dorsal portions of the esophagus during E11.5–E12.0 was 0.1501, and this difference was not statistically significant (permutation 10,000 rounds in MorphoJ:  $P > 0.6949$ ).

At E12.5–E13.0, the histograms and MDS 2D graphs again appeared to be quite similar between the ventral and dorsal regions of the esophagus (Fig. 4C, D). The scatter plot from CV1 and CV2 showed that two groups were overlapped (Fig. 5C). The Procrustes distance obtained by pairwise comparison among groups, E12.5–E13.0 esophagus ventral *vs.* dorsal, was 0.1568, and this difference was not statistically significant (permutation 10,000 rounds in MorphoJ:  $P > 0.6021$ ).

### **Convergent extension (CE): Measurement of total cell distributions along the L axis of the trachea and esophagus**

The convergent extension is a basic conserved cellular movement that forms elongated tissues across different species during embryonic development.<sup>19,20</sup> Here, we examined the

12 hr interval difference in cell distribution along the L axis to investigate whether CE was involved in the elongation of the trachea and esophagus. We compared the total cell distribution along the L axis at two time points (1 hr vs. 12 hr after EdU injection) for both E11.5 and E12.5. We set the cell distribution on the section on the X axis, and the length of the epithelial tube along the L axis on the Y axis. We then analyzed whether changes occurred along both axes of the epithelial tube. Between E11.5 and E12.0 (12 hr later), we observed that the short and thick tracheal and esophageal epithelial tubes became thin and long with a time course suggesting the existence of CE (Fig. 6A, B). Between E12.5 and E13.0, both epithelial tubes became slightly thicker and moderately longer, suggesting that CE did not take place (Fig. 6C, D). Therefore, CE is not likely involved in the elongation of the trachea or esophagus during E12.5–E13.0.

### **PCM along the L axis: % of EdU-positive nuclei distributions**

Cell movement and cell proliferation are equally important phenomena during the early embryonic development of organisms.<sup>21,22,27</sup> Thus, to analyze the PCM, i.e. cell movement along the L axis, we plotted the distribution of EdU-positive nuclei and EdU-negative nuclei on a graph and examined whether the ratio of the EdU-positive nuclei changes at the relative same position along the L axis after 12 hr. We assumed that if there is no PCM the distribution of the ratio of the EdU-positive nuclei along relative 100% length of the L axis would not change irrespective of the growth. The same embryonic day samples for CE analysis were used. The vertical Y-value represented the length of the organs in  $\mu\text{m}$  and the horizontal X-value represented the EdU-positive plus EdU-negative nuclei distribution (Fig. 7A, C). Then we further set up the % relative length vs. the % EdU-positive nuclei distribution graph (100

X 100) to examine whether there was a distribution change that suggested PCM of EdU (+) nuclei along the L axis (Fig. 7B, D).

Regarding the trachea, E11.5 (1 hr) vs. E12.0 (12 hr), the % of EdU-positive nuclei were in general uniformly distributed along the L axis (Fig. 7A). However, whereas the ratio of EdU-positive nuclei at E11.5 was relatively equal throughout the entire length, at E12.0 the ratio tended to be higher in the rostral half and lower in the caudal half than at E11.5 (Fig. 7B). In contrast, whereas the ratio of EdU-positive nuclei at E12.5 (1 hr) was again relatively equal throughout the entire length, at E13.0 (12 hr) the ratio of labeled EdU nuclei tended to be lower in the rostral half than at E12.5 (Fig. 7D).

Regarding the esophagus, between E11.5 and E12.0 the % of EdU-positive nuclei overlapped through the examined length (Fig. 8B). While at E11.5 (1 hr) the ratio tended to gradually increase from the rostral to caudal part, at E12.0 (12 hr) the ratio became rather irregular, higher in some parts and lower in the others (Fig. 8B). In the E12.5 (1 hr) esophagus, the % of EdU-positive nuclei tended to increase from the rostral to caudal part, while at E13.0 (12 hr) the ratio tended to be lower in the middle and higher in the rostral-most and caudal-most parts than at E12.5 (Fig. 8D). These findings of differences in the distribution of the % of EdU-positive nuclei along the L axis between the two time points with a 12 hr interval might suggest that PCM occurred from E11.5 to E13.0 both in the trachea and esophagus. However, we could not find a statistically significant difference either in the trachea or in the esophagus. These data are indirect and limited, and the existence of PCM remains to be confirmed.

## DISCUSSION

### Developmental significance of the difference in the modes of INM

INM is the AB polarity-based regulatory mechanism of proliferation and differentiation of the epithelial stem/progenitor cells, and the molecular mechanisms involving the cytoskeletal elements, albeit variable depending on the cases, have been suggested.<sup>5-11</sup> INM has been extensively studied in the neural ectoderm-derived epithelium and is considered the hallmark of neurogenesis; however, recent studies revealed that INM is also the main feature of other pseudostratified epithelial tubular tissues/organs of all three germ-layer origins in the embryo.<sup>9,16,28-30</sup> We also previously proved the existence of INM in endoderm-derived epithelia of the trachea and esophagus during E11.5–E12.0, in endoderm-derived epithelia of the entire intestine during E11.5–E14.0, and in the mesoderm-derived epithelium of the ureter during E11.5–E14.0.<sup>12-15</sup>

The basal-to-apical nuclear movement in the INM corresponds to G2/M phase and the apical-to-basal shift corresponds to G1 phase of the cell cycle.<sup>6-9</sup> Previous studies, including ours, revealed that the duration of the G1 phase nuclear shift varies significantly depending on the organs as well as on the developmental dates, whereas the G2/M phase shift is within a narrow time window and almost constant in each organ irrespective of dates.<sup>16,31,32</sup>

In the neural progenitor cells in the developing neocortex, the total INM cycle number has been calculated as 11, and the length of the overall cell cycle is approximately doubled over the interval from E11 to E16 due to the increase in the length of the G1 phase.<sup>31</sup> INM regulates not only proliferation of stem/progenitor cells but also differentiation of different types of daughter cells.<sup>33</sup> Therefore, through regulation of the fraction of the neural progenitor cell population that exits the cell cycle (Q fraction) at a given point of

neurogenesis, INM regulates not only the total neuron number/brain size, and thus the overall functional capacity of the brain, but also the layer distribution of different types of projection neurons in different regions,<sup>32</sup> and thereby, in theory, differential functions in different regions of the cerebral cortex.

We also previously documented regionally different INM modes in the intestine.<sup>15</sup> In the proximal intestine that later develops into the small intestine, the basal-to-apical and apical-to-basal movements of the nuclei take 4 hr and 8 hr, respectively, whereas in the distal intestine that corresponds to the future large intestine they require 6 hr and 2 hr, respectively.<sup>15</sup>

Thus, differential INM modes have been suggested to play an important role in the differential organogenesis and histogenesis of organs as well as in different regions of individual organs, and thereby in the differential structures and functions of organ regions.

We previously showed the existence of INM in the esophagus and trachea during E11.5–E12.0, and showed that INM ceases at an earlier time point in the esophagus, ranging from E13.0 to E14.0, while it continues until at least E14.0 in the trachea<sup>3,12</sup> as well as in other organs.<sup>13–15</sup> In the present study, using statistical analyses of the chronological change in the distribution pattern along the AB axis of the EdU-labeled epithelial nuclei, a method established in our previous series of studies,<sup>12–15</sup> we proved that there is a significant difference in the INM mode between the trachea and esophagus during E11.5–E12.0, but not between E12.5–E13.0. We further documented a significant regional difference in the INM mode between the dorsal and ventral sides of the E11.5–E12.0 trachea, but not in those during E12.5–E13.0, and not in the esophagus. These findings support our hypothesis on the existence of different modes of INM between the two organs which derive from the common

anterior foregut as well as between the dorsal and ventral sides of the trachea. These differences in the INM mode, albeit during the limited time period immediately after the separation of the two organs, may be related with the later differential organogenesis and histogenesis between the two organs as well as between the dorsal and ventral sides of the trachea.

Given the significance of the determined INM cycle number in the brain for regulating “normal” brain size, the other epithelial tubular organs with certain variable sizes within “normal” range are also assumed to have specifically determined INM cycle numbers, a hypothesis which requires further detailed investigation.

Further, the histograms of the EdU-positive nuclei distribution along the AB axis of the trachea and esophagus in the present study and those of the intestine<sup>14,15</sup> and ureter<sup>13</sup> in our previous studies all suggest that the nuclei are not all actively/continuously involved in the INM/cell cycle, but rather a significant part of the nuclei remain in the same position along the AB axis throughout the 12 hr interval. For example, in the present Fig. 2B, layer 2 has the highest EdU-positive nuclei ratio at all time points, indicating that a significant number of cell nuclei did not move along the AB axis during this time period, and the different patterns of histograms in the examined organs suggest that the ratio of the nuclei actively involved in INM differs depending on the organ/region and developmental date. To elucidate the actual contribution of INM to the resultant total cell number in the organ/region, the ratios of the cells that are actively involved in INM must be elucidated, which is currently under investigation in our laboratory.

## **CE and PCM along the L axis**

The process of CE, in which the epithelial tissue converges (narrows) toward the central axis and extends (lengthens) along the perpendicular axis, was first recognized as a morphogenetic process more than 100 years ago.<sup>19</sup> We previously reported that CE plays a role in elongation of the endoderm-derived midgut epithelium in humans<sup>17</sup> and in mice.<sup>18</sup> We further showed that Ror2, a receptor tyrosine kinase for Wnt5a, is expressed in the midgut epithelium and that, based on a Ror2-knockout study in mice, Ror2-mediated signaling is involved in the CE of the epithelium in the midgut elongation in mice.<sup>18</sup> Therefore, the midgut elongation appears to be an epithelium-driven phenomenon. Moreover, since the midgut epithelium is “single” columnar, CE in the midgut is not a polarized cell “rearrangement” but a polarized cell “transformation” and must involve cytoskeletal regulation in order to reduce the cell height along the AB axis of the “pseudostratified single columnar” epithelial cells, and thus this transformation is strongly suggested to be closely related with INM, the AB polarity-based cytoskeleton-related regulatory mechanism (Fig. S1).

In the present study, based on the chronological change over 12 h—i.e., a single cell cycle interval—in the cell distribution along the L axis, in different individuals, we observed the elongation and simultaneous narrowing of the epithelial tube of the trachea and esophagus, suggesting that CE is involved in their elongation. On the other hand, Kishimoto et al. showed that the diameter of the trachea including the surrounding mesenchyme remains almost the same from E10.5 to E14.5, and further that Ror2 is not expressed in the epithelia of the trachea or esophagus and Wnt5a-Ror2 signaling in the mesenchyme actively regulates the elongation of the tube.<sup>34</sup> We observed CE and INM in the epithelia of the trachea and

esophagus in the present study, as well as in the midgut in our previous study.<sup>14,18</sup> In the trachea and esophagus, since Ror2 is not expressed in the epithelium, only the primary mesenchymal Ror2-mediated signal secondarily could mediate and induce CE, the epithelial cell transformation. This apparent discrepancy in the elongation between the trachea/esophagus and midgut, different parts of the continuous endoderm-derived gut, give rise to at least two hypotheses. First, the mechanism involved in the tube elongation may differ between organs. In this case, the possible regulation of CE/INM is either originated endogenously in the epithelium or induced secondarily by the signals from the surrounding mesenchyme. Second, since Ror2 is expressed not only in the midgut epithelium but also the surrounding mesenchyme, albeit more weakly than in the epithelium,<sup>18</sup> the primary signal might also be generated in the mesenchyme in the midgut (Fig. S2). Intriguingly, even within the midgut, there are regional and differential differences in the expression patterns of Ror2 and Wnt5a,<sup>18</sup> and therefore, further detailed analysis is warranted on the interaction between the epithelium and mesenchyme via Wnt5a/Ror2 signaling and others.

PCM, the cell movement under PCP, causes a change in the cell distribution along the L axis and thereby affects the organogenesis of the tubular tissues/organs.<sup>21,22</sup> In the present study, we only examined chronological change over a 12 hr interval in the distribution of the ratio of the EdU-positive nuclei along the L axis, again based on data from different individuals, assuming that if there is no PCM this distribution does not change. Although we observed some changes in the trachea or esophagus, none rose to the level of statistical significance. PCM causes collective cell migration along the L axis, and thus regional differences in the PCM mode/magnitude could affect the morphogenesis/organogenesis of the tube.<sup>22</sup> The PCP pathway has also been implicated in the directional movement of individual cells.<sup>21</sup> In the

developing lung epithelium, pulmonary neuroendocrine (NE) cells, the production of which, by analogy in the brain to produce neuroblasts, could be related with INM, have been shown to be generated and to undergo directional migration mostly in the distal direction toward the bifurcation points.<sup>35</sup> This PCM may affect the cell distribution along the L axis and thus, at least in part, the morphogenesis of the tube.

In conclusion, in the present study, we observed an inter-organ difference in the INM mode between the trachea and esophagus, and an intra-regional (dorsal vs. ventral) difference in the trachea, both during E11.5–E12.0. We further showed that CE occurs in both organs during E11.5–E12.0. These cellular events may be involved in the differential normal and abnormal organogenesis and later histogenesis of these two organs.

## **ACKNOWLEDGMENTS**

We would like to extend our deep appreciation to Ms. Y. Takeda for her tireless assistance with the tissue sectioning. This work was supported by MEXT KAKENHI Grant Number 23112006.

**DISCLOSURE:** None.

## REFERENCES

1. Morrisey EE, Hogan BL. Preparing for the first breath: genetic and cellular mechanisms in lung development. *Dev Cell.* 2010;18(1):8-23.
2. Wong NC, Armin P, Jiang M, Ku W-Y, Jacobs I, Que J. Chapter 17 - SOX2 in the Development and Maintenance of the Trachea, Lung, and Esophagus. In: Kondoh H, Lovell-Badge R, eds. *Sox2*. Boston: Academic Press; 2016:301-319.
3. Getachew D, Kaneda R, Saeki Y, Matsumoto A, Otani H. Morphologic changes in the cytoskeleton and adhesion apparatus during the conversion from pseudostratified single columnar to stratified squamous epithelium in the developing mouse esophagus. *Congenit Anom (Kyoto).* 2020;1–11. <https://doi.org/10.1111/cga.12389>.
4. Grosse AS, Pressprich MF, Curley LB, et al. Cell dynamics in fetal intestinal epithelium: implications for intestinal growth and morphogenesis. *Development.* 2011;138(20):4423-4432.
5. Norden C, Young S, Link BA, Harris WA. Actomyosin is the main driver of interkinetic nuclear migration in the retina. *Cell.* 2009;138(6):1195-1208.
6. Del Bene F. Interkinetic nuclear migration: cell cycle on the move. *EMBO J.* 2011;30(9):1676-1677.
7. Spear PC, Erickson CA. Interkinetic Nuclear Migration: A Mysterious Process in Search of a Function. *Dev Growth Differ.* 2012;54(3):306-316.

8. Kosodo Y, Suetsugu T, Suda M, et al. Regulation of interkinetic nuclear migration by cell cycle-coupled active and passive mechanisms in the developing brain. *EMBO J.* 2011;30(9):1690-1704.
9. Kosodo Y. Interkinetic nuclear migration: beyond a hallmark of neurogenesis. *Cell Mol Life Sci.* 2012;69(16):2727-2738.
10. Taverna E, Huttner WB. Neural progenitor nuclei IN motion. *Neuron.* 2010;67(6):906-914.
11. Del Bene F, Wehman AM, Link BA, Baier H. Regulation of neurogenesis by interkinetic nuclear migration through an apical-basal notch gradient. *Cell.* 2008;134(6):1055-1065.
12. Kaneda R, Saeki Y, Getachew D, et al. Interkinetic nuclear migration in the tracheal and esophageal epithelia of the mouse embryo: Possible implications for tracheo-esophageal anomalies. *Congenit Anom (Kyoto).* 2018;58(2):62-70.
13. Motoya T, Ogawa N, Nitta T, et al. Interkinetic nuclear migration in the mouse embryonic ureteric epithelium: Possible implication for congenital anomalies of the kidney and urinary tract. *Congenit Anom (Kyoto).* 2016;56(3):127-134.
14. Yamada M, Udagawa J, Hashimoto R, Matsumoto A, Hatta T, Otani H. Interkinetic nuclear migration during early development of midgut and ureteric epithelia. *Anat Sci Int.* 2013;88(1):31-37.
15. Nitta T, Ogawa N, Getachew D, Matsumoto A, Udagawa J, Otani H. Spatiotemporal Difference in the Mode of Interkinetic Nuclear Migration in the Mouse Embryonic Intestinal Epithelium. *Shimane J Med Sci.* 2017;33(2):79-85.

16. Otani H, Udagawa J, Naito K. Statistical analyses in trials for the comprehensive understanding of organogenesis and histogenesis in humans and mice. *J Biochem* 2016;159(6):553-561.
17. Matsumoto A, Hashimoto K, Yoshioka T, Otani H. Occlusion and subsequent re-canalization in early duodenal development of human embryos: integrated organogenesis and histogenesis through a possible epithelial-mesenchymal interaction. *Anat Embryol (Berl)*. 2002;205(1):53-65.
18. Yamada M, Udagawa J, Matsumoto A, et al. Ror2 is required for midgut elongation during mouse development. *Dev Dyn*. 2010;239(3):941-953.
19. Wallingford JB, Fraser SE, Harland RM. Convergent extension: the molecular control of polarized cell movement during embryonic development. *Dev Cell*. 2002;2(6):695-706.
20. Shindo A. Models of convergent extension during morphogenesis. *Wiley Interdiscip Rev Dev Biol*. 2018;7(1):e293.
21. Davey CF, Moens CB. Planar cell polarity in moving cells: think globally, act locally. *Development*. 2017;144(2):187-200.
22. Henderson DJ, Long DA, Dean CH. Planar cell polarity in organ formation. *Curr Opin Cell Biol*. 2018;55:96-103.
23. Shinkareva SV, Wang J, Wedell DH. Examining Similarity Structure: Multidimensional Scaling and Related Approaches in Neuroimaging. *Comput Math Methods Med*. 2013;2013:9.

24. Udagawa J, Yasuda A, Naito K, Otani H. Analysis of the harmonized growth pattern of fetal organs by multidimensional scaling and hierarchical clustering. *Congenit Anom (Kyoto)*. 2010;50(3):175-185.
25. Klingenberg C. MorphoJ: an integrated software package for geometric morphometrics. *Mol Ecol Resour*. 2011;11(2):353-357.
26. Sontigun N, Sukontason KL, Zajac BK, et al. Wing morphometrics as a tool in species identification of forensically important blow flies of Thailand. *Parasit Vectors*. 2017;10(1):229-229.
27. Halacheva V, Fuchs M, Dönitz J, Reupke T, Püschel B, Viebahn C. Planar cell movements and oriented cell division during early primitive streak formation in the mammalian embryo. *Dev Dyn*. 2011;240(8):1905-1916.
28. Miyata T, Okamoto M, Shinoda T, Kawaguchi A. Interkinetic nuclear migration generates and opposes ventricular-zone crowding: insight into tissue mechanics. *Front Cell Neurosci*. 2015;8(473).
29. Meyer EJ, Ikmi A, Gibson MC. Interkinetic nuclear migration is a broadly conserved feature of cell division in pseudostratified epithelia. *Curr Biol*. 2011;21(6):485-491.
30. Fousse J, Gautier E, Patti D, Dehay C. Developmental changes in interkinetic nuclear migration dynamics with respect to cell-cycle progression in the mouse cerebral cortex ventricular zone. *J Comp Neurol*. 2019;527(10):1545-1557.
31. Takahashi T, Nowakowski RS, Caviness VS. The cell cycle of the pseudostratified ventricular epithelium of the embryonic murine cerebral wall. *J Neurosci*. 1995;15(9):6046-6057.

32. Mitsuhashi T, Takahashi T. Genetic regulation of proliferation/differentiation characteristics of neural progenitor cells in the developing neocortex. *Brain Dev.* 2009;31(7):553-557.
33. Willardsen MI, Link BA. Cell biological regulation of division fate in vertebrate neuroepithelial cells. *Dev Dyn.* 2011;240(8):1865-1879.
34. Kishimoto K, Tamura M, Nishita M, et al. Synchronized mesenchymal cell polarization and differentiation shape the formation of the murine trachea and esophagus. *Nat Commun.* 2018;9(1):2816.
35. Noguchi M, Sumiyama K, Morimoto M. Directed Migration of Pulmonary Neuroendocrine Cells toward Airway Branches Organizes the Stereotypic Location of Neuroepithelial Bodies. *Cell Rep.* 2015;13(12):2679-2686.

## FIGURE LEGENDS

Figure 1: The image processing program (A) which divides the epithelium layer into six equal concentric circles with 15° segments. We placed a dot at the center of the EdU-positive nuclei so that they could be assigned to the appropriate layer (L1–L6), with the basal side (basement membrane) considered as L1 and the apical side as L6 (4 hr esophagus, B). In the E11.5 trachea (D,E,F) and esophagus (G,H,I), EdU staining using a Click-iT EdU Alexa Fluor 488 Kit (Invitrogen) reveals the cyclic movement of the EdU-positive nuclei from basal-to-apical-to-basal at different time intervals (1, 4, and 12 hr). DNA synthesis nuclei are shown in green and DAPI nuclei in blue. The EdU-positive nuclei were shifted to the apical side at 4 hr and then returned to the basal side at 12 hr. The micrograph (C) shows the orientation of the ventral (v) and dorsal (d) sides of these organs at E11.5 plus 4 hr. Scale bars D–I: 20 μm.

Figure 2: The histogram of distribution of the percentage (%) of EdU-positive nuclei at each time point (left panels) and 2D MDS representation (right panels) of the E11.5 total trachea (A) vs. total esophagus (B), and E12.5 total trachea (C) vs. total esophagus (D). At E11.5 the numbers of EdU-positive nuclei counted were 5306 for the total trachea and 3679 for the total esophagus, whereas at E12.5 they were 8798 for the total trachea and 6876 for the total esophagus (1 hr–12 hr). At E11.5, the EdU-positive nuclei position shifted from the basal side at 1 hr to the apical side at 4 hr, then returned to the basal side at 12 hr in both organs. The cell cycle phase was completed at 12 hr for both the total trachea and total esophagus, whereas the mode of the cyclic pattern differed between the two organs. At E12.5, the EdU-positive nuclei were located on the basal side at 1 and 12 hr, whereas the time point of the shift to the apical side was 6 hr for both the total trachea total esophagus. The cell cycle phase

was completed at 12 hr for both the total trachea and total esophagus, while the mode of the INM cyclic pattern appeared somewhat different between the two organs. Bars indicate standard deviations. Beneath each MDS panel, changes in the Dimension 1 value (X-axis) are shown to represent the basal-to-pical side and apical-to-basal shifts of nuclear distribution.

Figure 3: The histogram of distribution of the percentage (%) of EdU-positive nuclei at each time point (left panels) and 2D MDS representation (right panels) of the E11.5 ventral trachea (A) vs. dorsal trachea (B) and E12.5 ventral trachea (C) vs. dorsal trachea (D). At E11.5, the EdU-positive nuclei shift to the apical side at 4 hr and back to the basal side at 12 hr both on the ventral and the dorsal side. At E12.5 the labeled nuclei shift to the apical side at 6 hr and back to the basal side at 12 hr both on the ventral and the dorsal side. The cell cycle phase was completed at 12 hr in all groups, whereas the mode of the cyclic pattern varied between the ventral and the dorsal side of the trachea at E11.5 Bars indicate standard deviations. Beneath each MDS panel, changes in the Dimension 1 value (X-axis) are shown to represent the basal-to-pical side and apical-to-basal shifts of nuclear distribution.

Figure 4: The histogram of distribution of the percentage (%) of EdU-positive nuclei at each time point (left panels) and 2D MDS representation (right panels) of E11.5 ventral esophagus (A) vs. dorsal esophagus (B), and E12.5 ventral esophagus (C) vs. dorsal esophagus (D). At E11.5, the EdU-labeled nuclei shift to the apical side at 4 hr and then back to the basal side at 12 hr both on the ventral and the dorsal side. 2D MDS patterns are generally similar between the ventral and dorsal sides. At E12.5, 2D MDS patterns are again generally similar between the ventral and dorsal sides, although the apical side shift at 4 hr and 6 hr somewhat

differs. Bars indicate the standard deviations. Beneath each MDS panel, changes in the Dimension 1 value (X-axis) are shown to represent the basal-to pical side and apical-to-basal shifts of nuclear distribution.

Figure 5: Scatter plot (A, B, C) showing the variation in shape of the total trachea vs. total esophagus at E11.5 and E12.5 (A), ventral vs. dorsal trachea at E11.5 and E12.5 (B), and ventral vs. dorsal esophagus at E11.5 and E12.5 (C). The first two canonical variate analysis, CV1 and CV2 axes counted for 95.56%, 98.40%, 98.81% confidence ellipses, respectively. At E11.5 the shape of the total trachea was separated from that of the total esophagus while at E12.5 the two shapes were overlapped in the CV2 direction (A). At E11.5 the shape of the ventral trachea was separate from the shape of the dorsal trachea, whereas at E12.5 the two shapes overlapped in the CV1 direction (B). The shape of the ventral esophagus overlapped that of the dorsal esophagus both in the CV1 and CV2 directions, and both at E11.5 and E12.5. This indicates that the ventral and the dorsal side of the esophagus appeared to be similar.

Figure 6: Convergent extension (CE) at the E11.5 trachea (A) and esophagus (B) at 1 hr vs. 12 hr. CE appeared to take place because the short and thick trachea changed into a long and thin epithelial tube over the period of observation. The comparisons of the E12.5 trachea (C) and esophagus (D) between 1 hr and 12 hr suggest that the CE did not take place along the long axis.

Figure 7: EdU-positive nuclei distribution to examine a possible Planar cell movement (PCM) in the E11.5 (A, B) and E12.5 trachea (C, D). Cell numbers along the measured length (A, C) and % ratio of EdU-positive nuclei along the relative length (B, D) are shown. At E11.5 (A) and E12.5 (C), the EdU-positive nuclei were in general uniformly distributed. At both E11.5 and E12.5, distributions of EdU-positive nuclei after 12 hr appeared somewhat different from those at 1 hr. While this result might suggest that PCM took place in the development of trachea, we could not find a statistically significant difference.

Figure 8: EdU-positive nuclei distribution to examine a possible Planar cell movement (PCM) in the E11.5 (A, B) and E12.5 esophagus (C, D). Cell numbers along the measured length (A, C) and % ratio of EdU-positive nuclei along the relative length (B, D) are shown. At E11.5 (A), the EdU-positive nuclei were in general uniformly distributed, and at E12.5 (C), EdU-positive nuclei distribution tended to be higher in the distal part. At both E11.5 and E12.5, distributions of EdU-positive nuclei after 12 hr appeared somewhat different from those at 1 hr. While this result might suggest that PCM took place in the development of esophagus, we could not find a statistically significant difference.

Figure S1: Polarized transformation of the epithelia cells causes CE. Pseudostratified single-layered columnar epithelium changes into simple mono-layered epithelium via the transformation of epithelial cells driven by the cytoskeleton along the AB axis causing intercalation of the nuclei and the resultant CE/elongation of the tube. Since this AB polarity-based transformation involves cytoskeleton, it should be also closely related with and modify INM, the AB-polarity-based cytoskeleton-related regulatory mechanism of the epithelial

progenitor cells. The modified INM would lead the change in the progenitor cell number, and, together with CE, would modify the organ shape and size.

Figure S2: Expression pattern of Ror2 in the epithelia and the surrounding mesenchyme in the trachea/esophagus (left) and the proximal midgut (right). In the trachea and esophagus, Wnt5a-Ror2 signaling in the mesenchyme primarily occurs and secondarily induce the events in the epithelium, because Ror2 is not expressed in the epithelium. In the midgut, Ror2 is expressed both in the epithelium and mesenchyme, and the primary Wnt5a-Ror2 signaling may occur either in the epithelium or in the mesenchyme. The darker shadow indicates the higher expression (arbitrary).

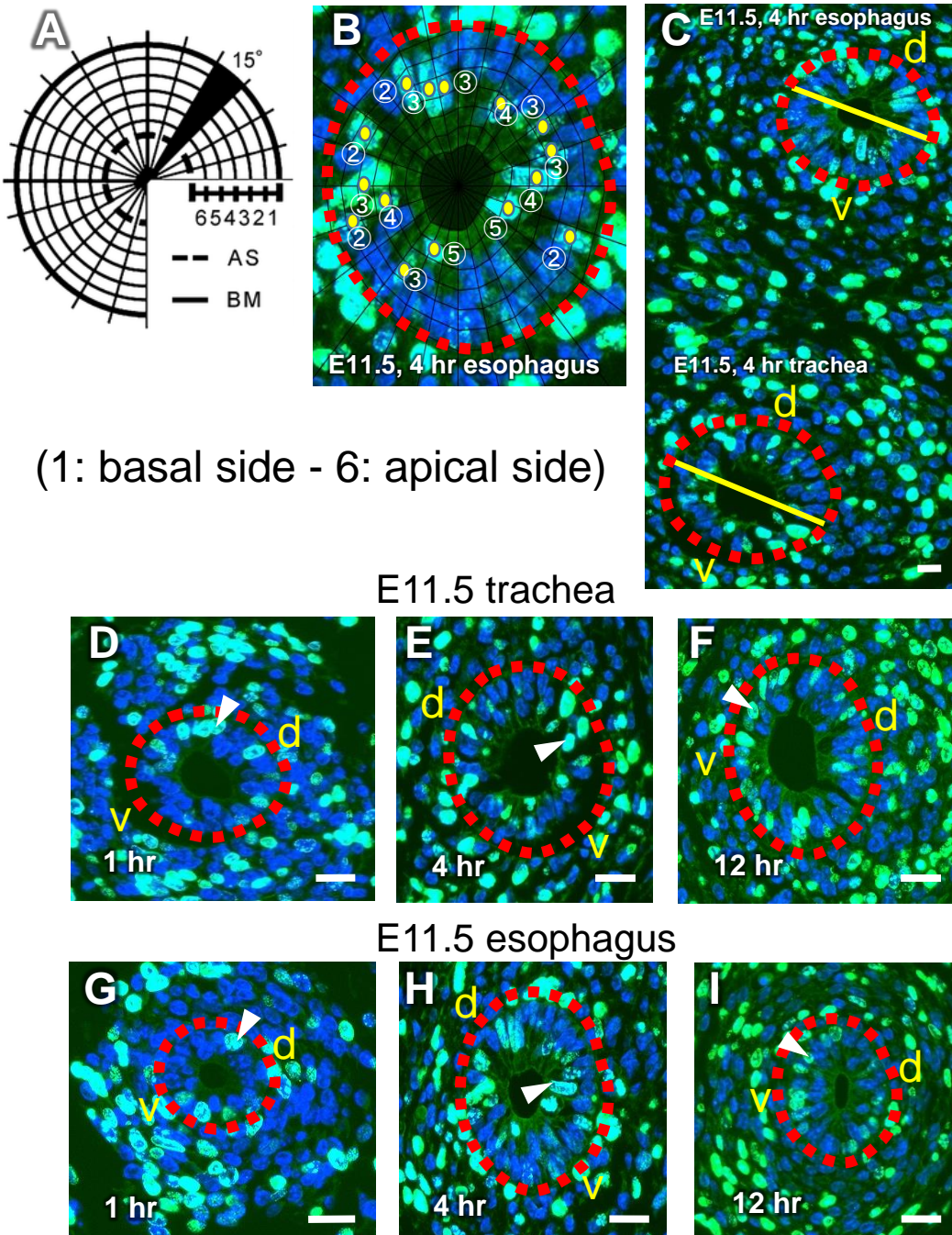


Figure 1

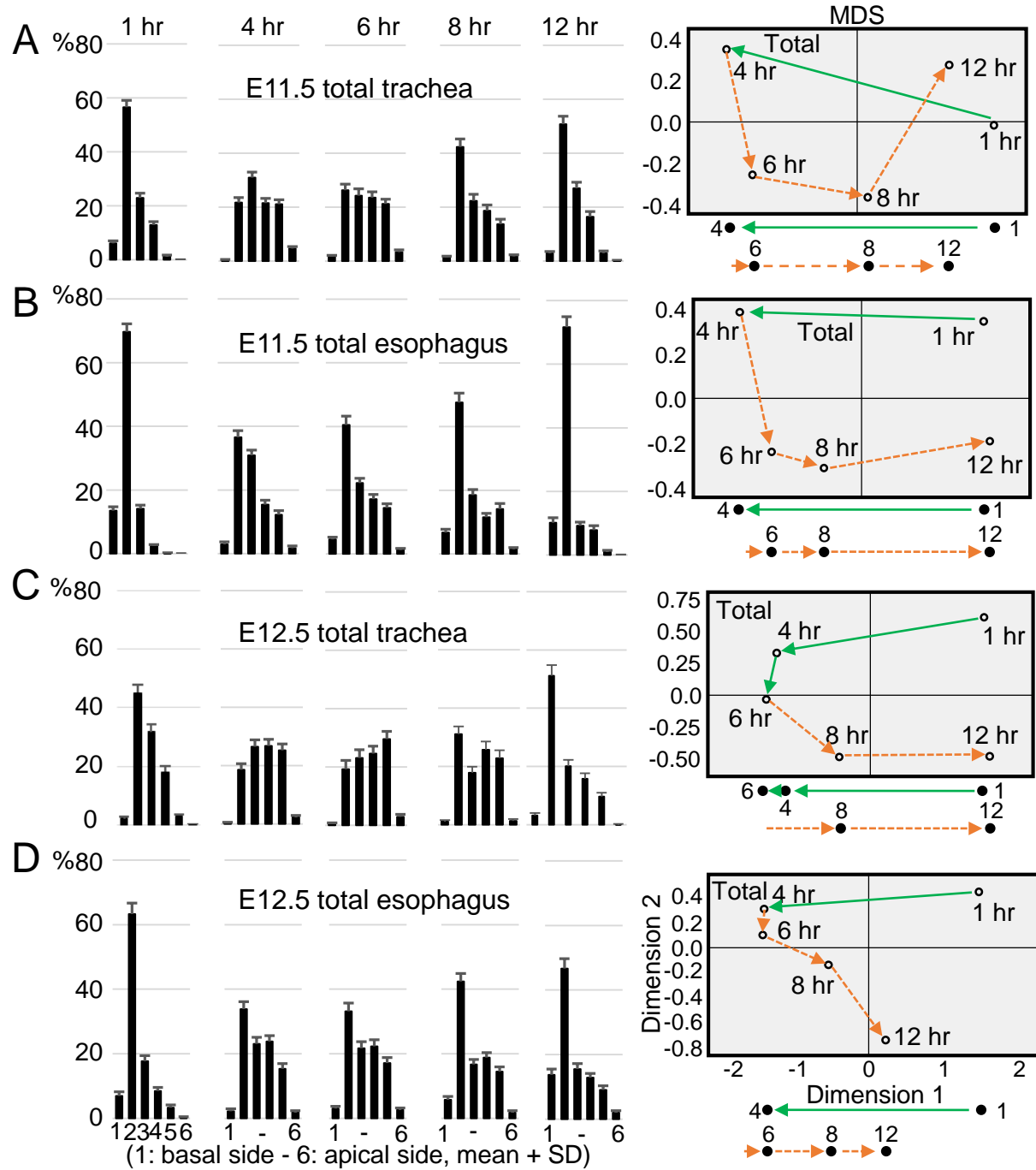


Figure 2

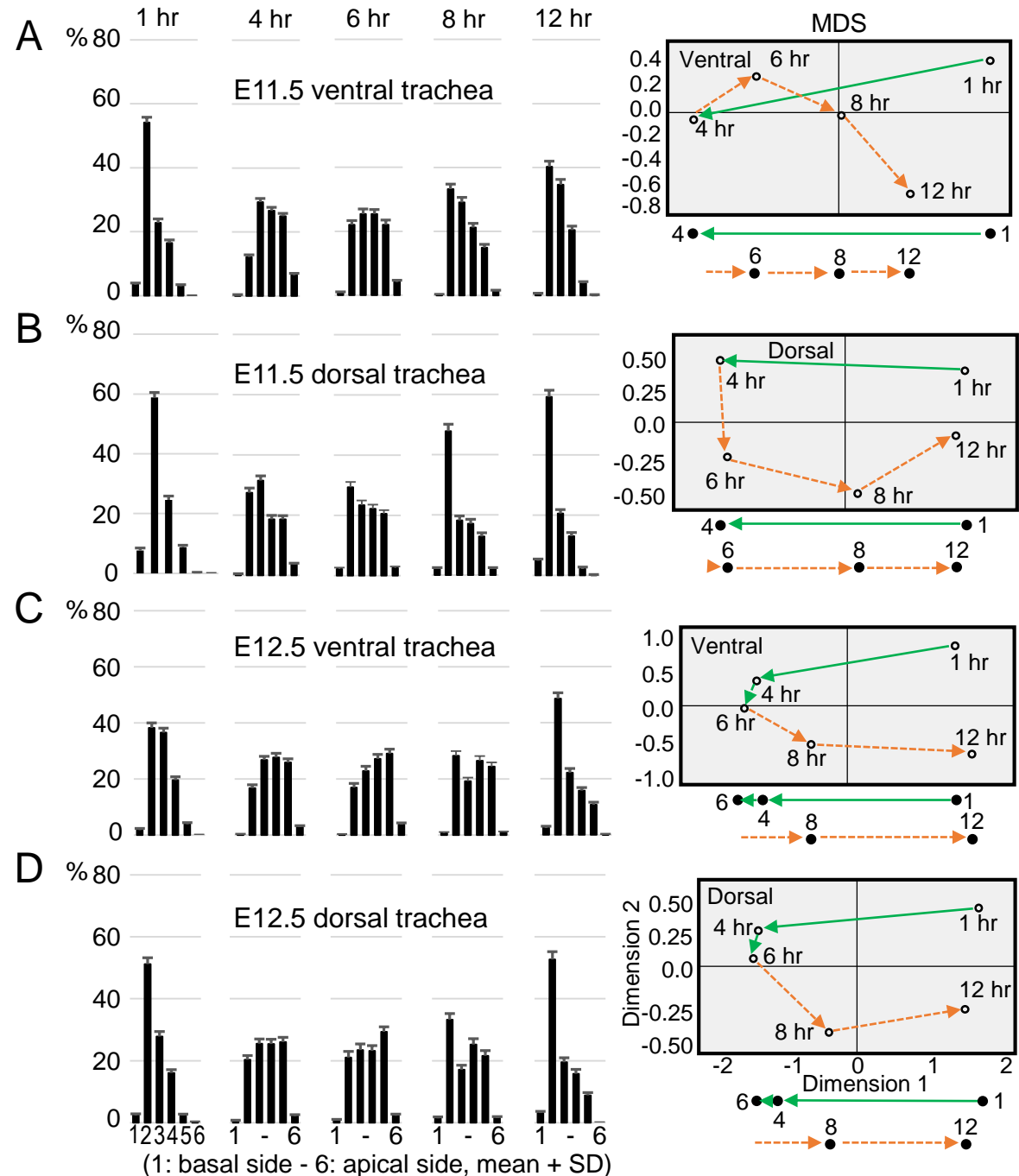


Figure 3

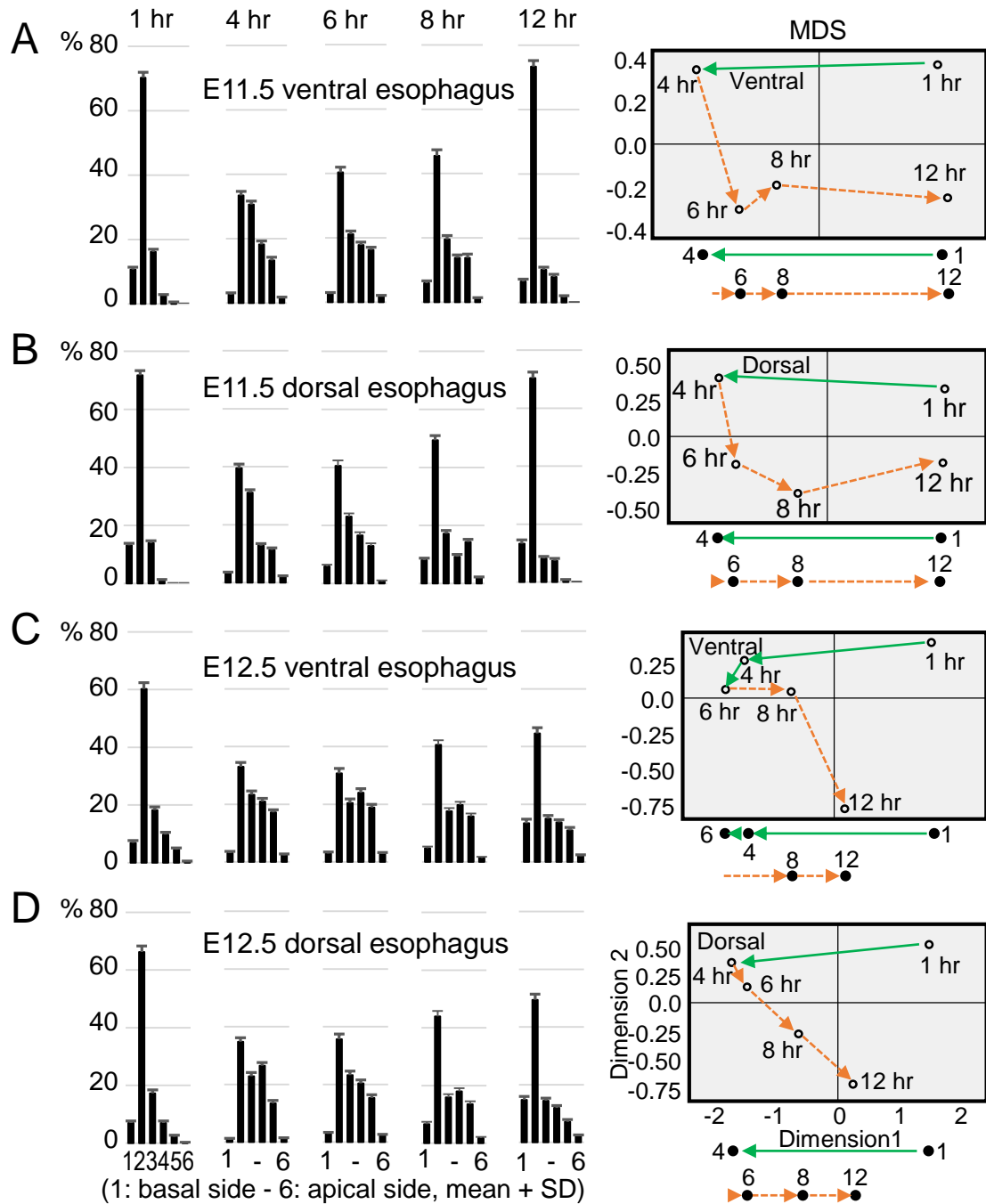


Figure 4

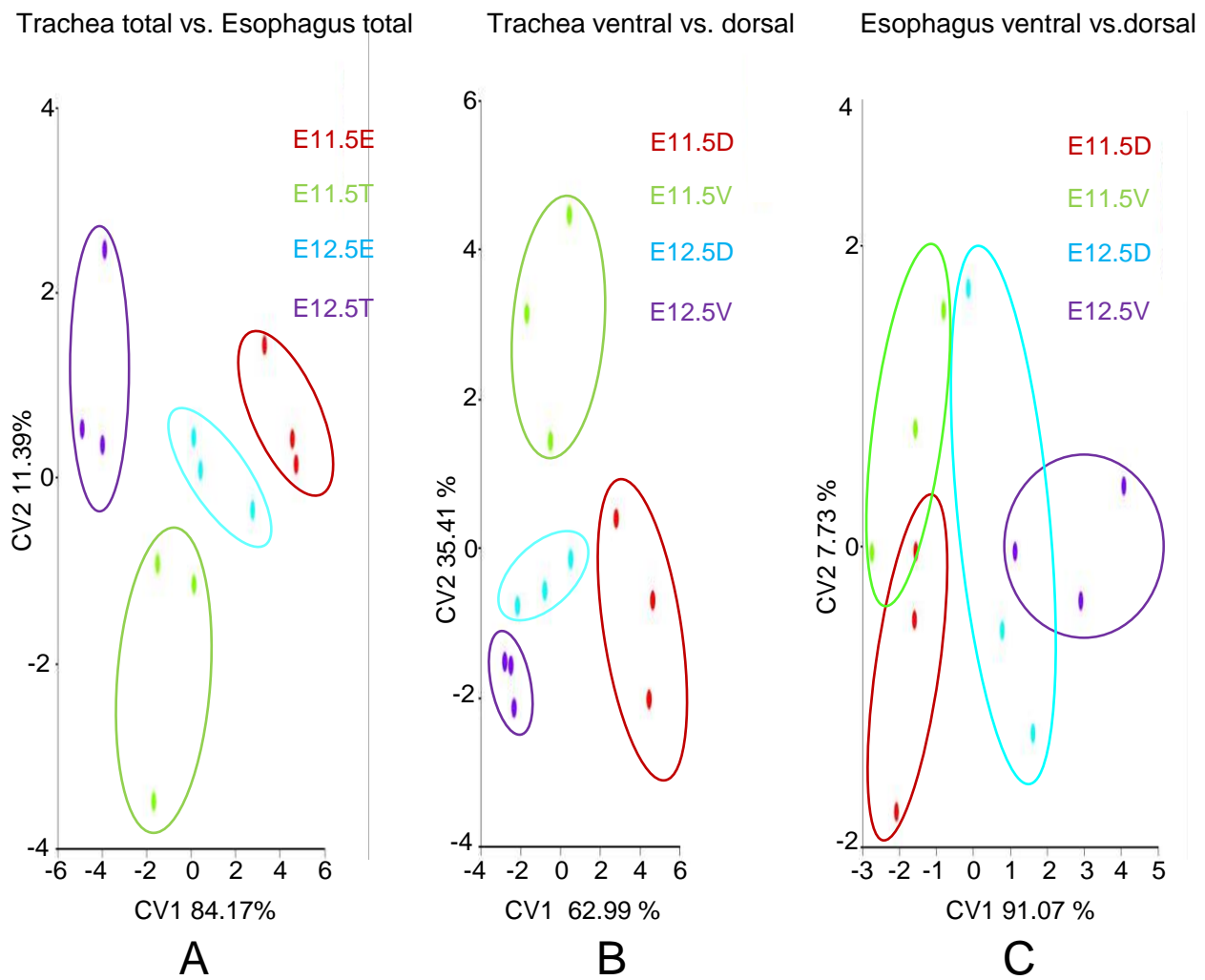
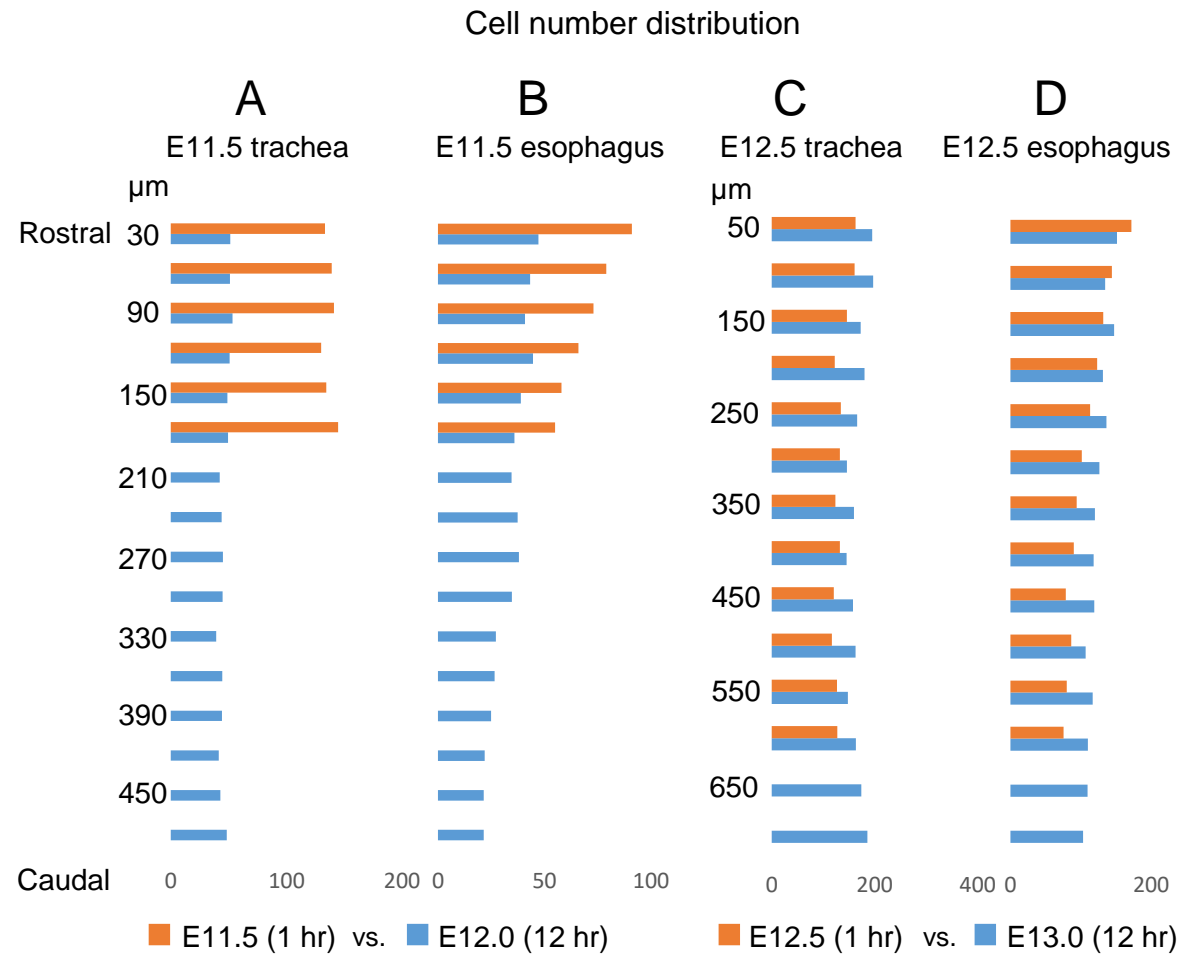


Figure 5



## Figure 6

### EdU (+/-) nuclei distribution in trachea

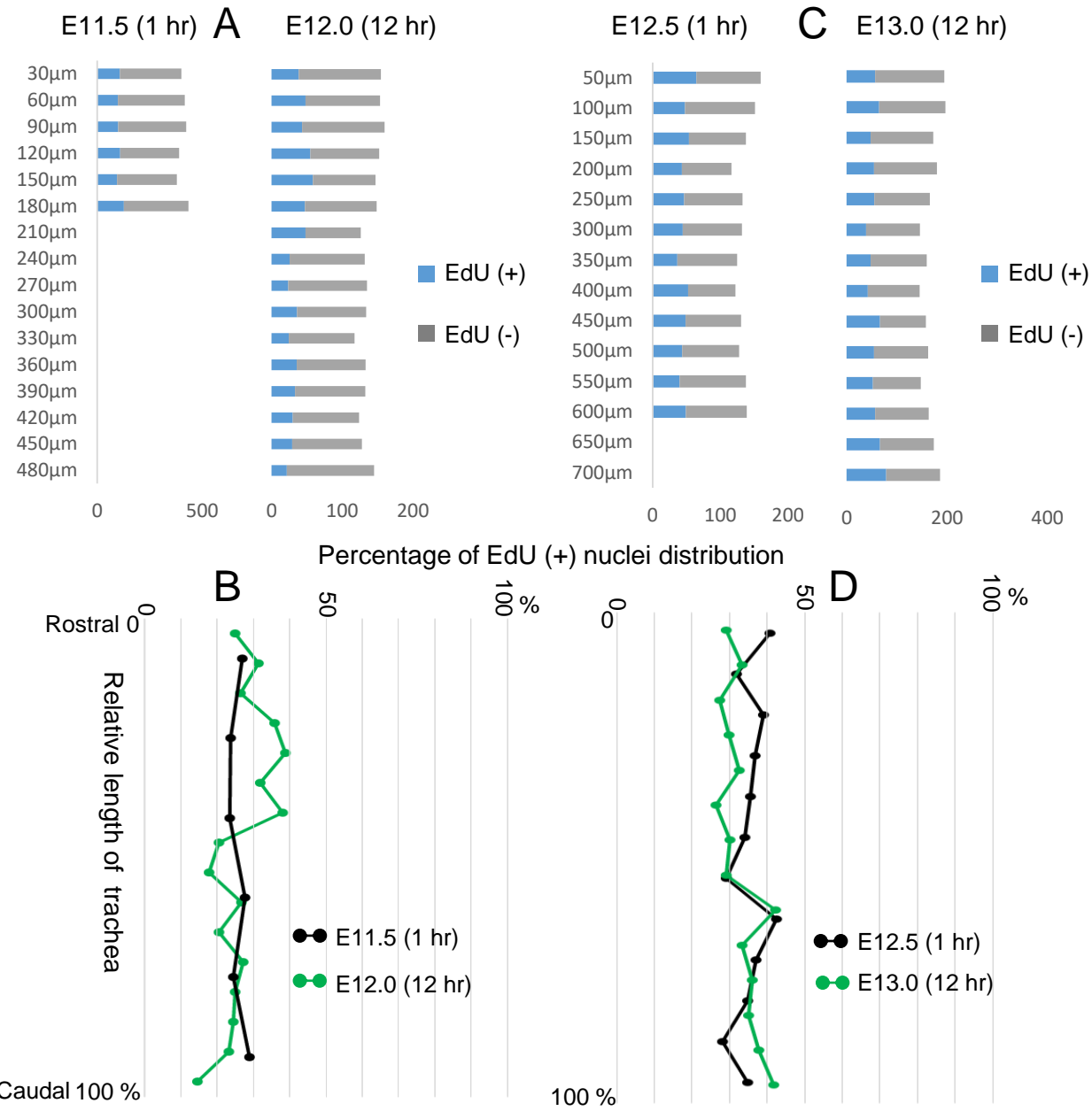


Figure 7

### EdU (+/-) nuclei distribution in esophagus

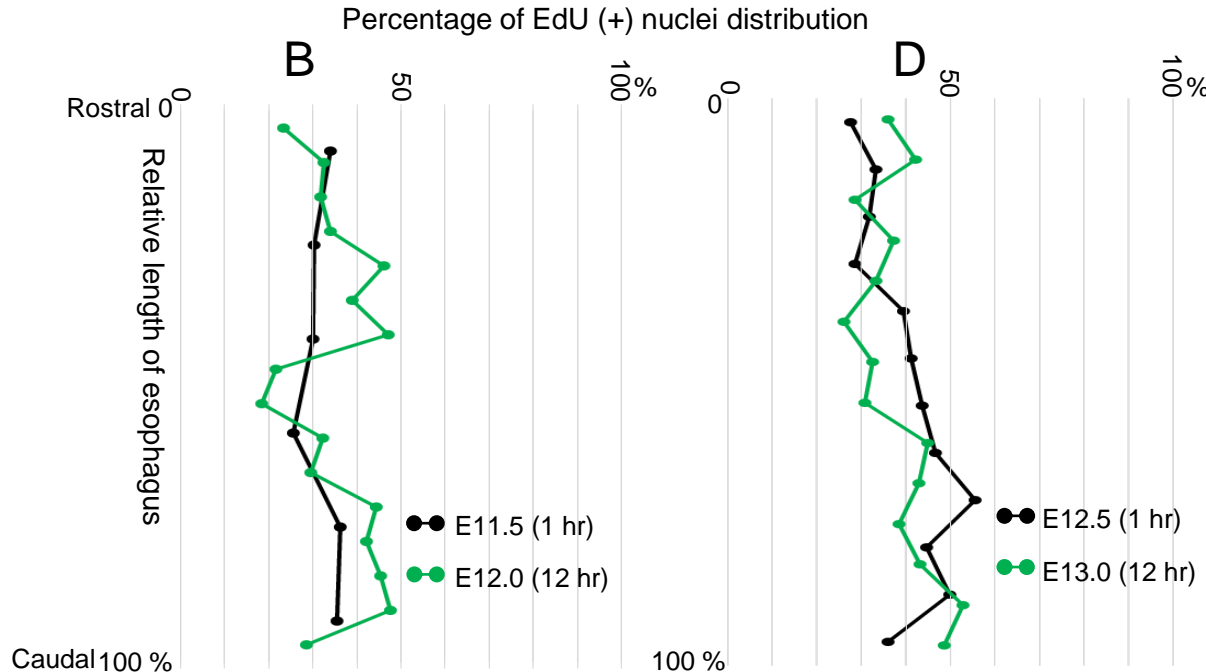
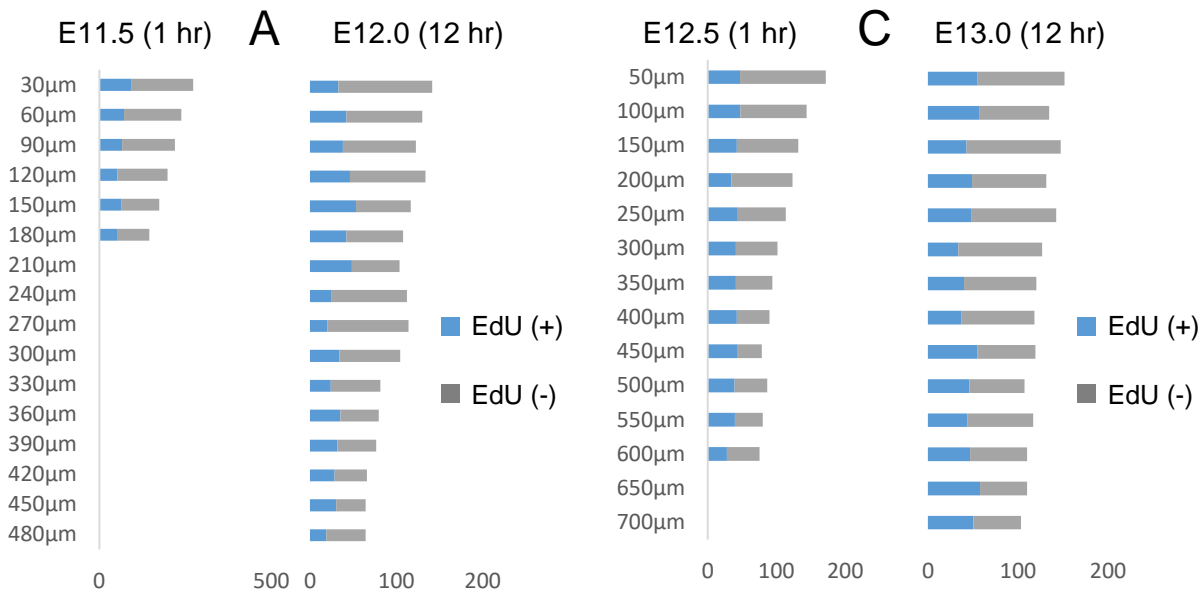
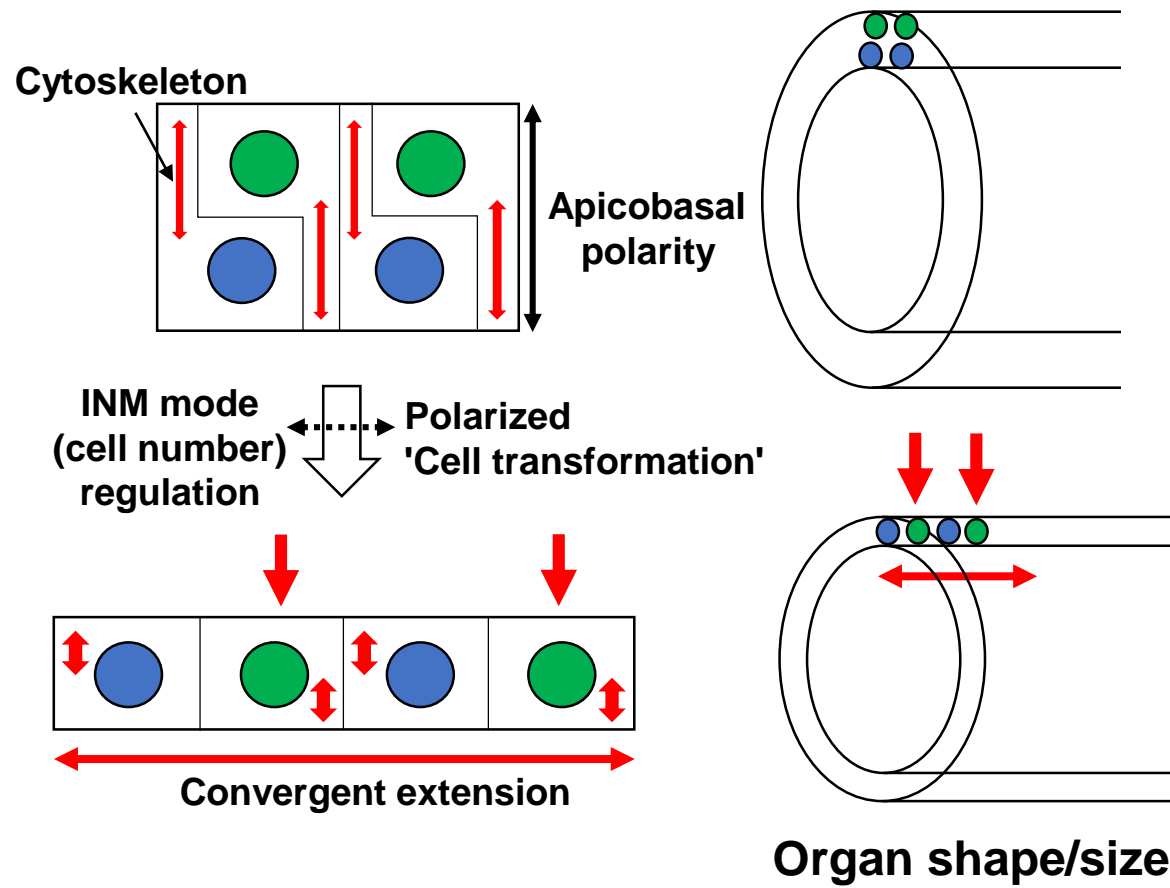


Figure 8

## Supporting Information



**Figure S1:** Polarized transformation of the epithelia cells causes CE. Pseudostratified single-layered columnar epithelium changes into simple mono-layered epithelium via the transformation of epithelial cells driven by the cytoskeleton along the AB axis causing intercalation of the nuclei and the resultant CE/elongation of the tube. Since this AB polarity-based transformation involves cytoskeleton, it should be also closely related with and modify INM, the AB-polarity-based cytoskeleton-related regulatory mechanism of the epithelial progenitor cells. The modified INM would lead the change in the progenitor cell number, and, together with CE, would modify the organ shape and size.

## Supporting Information

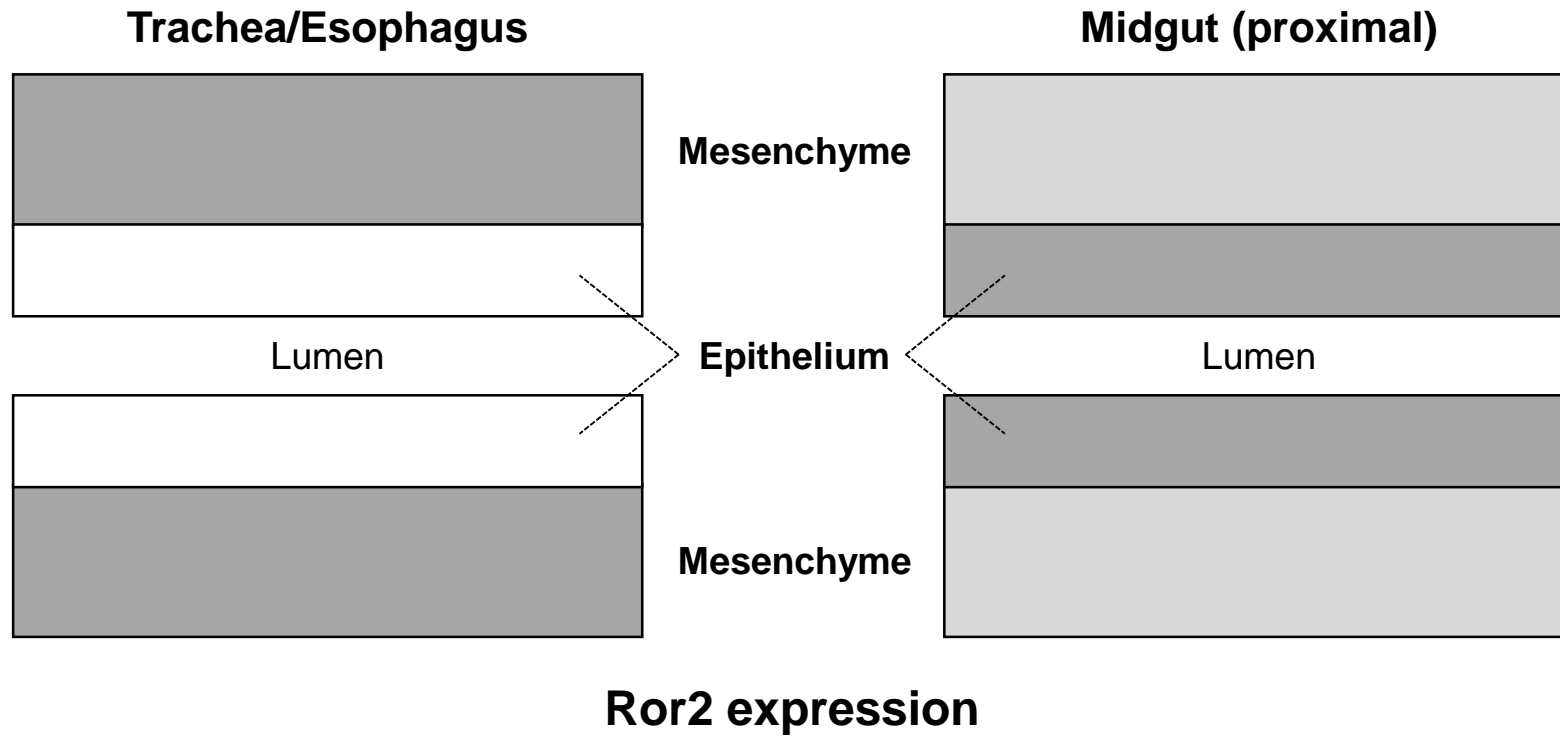


**Figure S2:** Expression pattern of Ror2 in the epithelia and the surrounding mesenchyme in the trachea/esophagus (left) and the proximal midgut (right). In the trachea and esophagus, Wnt5a-Ror2 signaling in the mesenchyme primarily occurs and secondarily induce the events in the epithelium, because Ror2 is not expressed in the epithelium. In the midgut, Ror2 is expressed both in the epithelium and mesenchyme, and the primary Wnt5a-Ror2 signaling may occur either in the epithelium or in the mesenchyme. The darker shadow indicates the higher expression (arbitrary).